Bioprocess Biosyst Eng (2014) 37:849–855
DOI 10.1007/s00449-013-1055-7

ORIGINAL PAPER

Real-time measurement of quorum-sensing signal autoinducer 3OC6HSL by a FRET-based nanosensor

Chang Zhang · Bang-Ce Ye

Received: 16 June 2013 / Accepted: 6 September 2013 / Published online: 22 September 2013

Abstract Quorum sensing (QS) is involved in many important biological functions such as luminescence, antibiotic production, and biofilm formation. The autoinducer *N*-(3-oxo-hexanoyl)-L-homoserine lactone (3OC6HSL) plays a significant role in the QS system of the marine bacterium *Vibrio fischeri*. Tracing 3OC6HSL would be significant in studies related to QS signal transduction. Traditional detection of QS signaling molecules has relied on bacterial reporter strains and high-performance liquid chromatography, which are time consuming and have low sensitivity. Because 3OC6HSL binding to LuxR from *V. fischeri* causes a conformational change, we developed a genetically encoded biosensor based on Förster resonance energy transfer (FRET) by inserting LuxR between the FRET pair YFP/CFP. The detection limit of the sensor was 100 μM. We attained an optimized sensor with 70 % Δratio increase by screening different hydrophobic linkers, and demonstrated the feasibility of this sensor for visualizing 3OC6HSL both in vitro and in vivo.

Keywords Genetically encoded biosensor · Quorum sensing · FRET · LuxR

Abbreviations

CFP	Cyan fluorescent protein
YFP	Yellow fluorescent protein
FLIP	Fluorescent indicator protein
FRET	Förster resonance energy transfer

Introduction

Bacterial cells sense the density of their population through a sophisticated cell–cell communication system and trigger the expression of various genes when the cell density reaches a specific threshold. This type of gene regulation, which controls diverse biological functions, including bioluminescence, antibiotic production, plasmid transfer, motility, virulence, and biofilm formation, is known as quorum sensing [1]. Understanding the quorum-sensing network would shed light on microbial metabolism and contribute to human health [2]. Recent research suggests that both prokaryotes [3, 4] and eukaryotes [5] possess interference strategies, which are used in natural settings to disrupt quorum sensing. These exciting findings on the QS-dependent behaviors of microorganisms, particularly the expression of virulence genes and biofilm formation, as well as the intensive concerns surrounding the rapidly increased incidence of antibiotic resistance [6], have become an important impetus for investigating practical approaches for interfering with microbial QS regulatory system. These approaches, also known as quorum quenching [7], have been explored as methods for preventing and controlling bacterial infection. One of the quorum quenching elements, *N*-acyl-homoserine lactonase (AiiA), is an enzyme that degrades *N*-acyl-homoserine lactone (AHL) molecules, and thus effectively interrupts pathogen communication. AHL-lactonase induces hydrolysis of the homoserine lactone ring

Electronic supplementary material The online version of this article (doi:10.1007/s00449-013-1055-7) contains supplementary material, which is available to authorized users.

C. Zhang · B.-C. Ye (✉)
Laboratory of Biosystems and Microanalysis, State Key Laboratory of Bioreactor Engineering, East China University of Science and Technology, Meilong Road 130, Shanghai 200237, China
e-mail: bcye@ecust.edu.cn

of AHL molecules. AHL-lactonase activity was first demonstrated in *Bacillus* sp. [8], which hydrolyzes a large range of AHL molecules.

The luminescence (lux) operon (*luxICDABEG*) of *Vibrio fischeri* is regulated by the transcriptional activator LuxR and 3OC6HSL [9, 10]. In this system, LuxI synthase enzymatically produces 3OC6HSL, which can diffuse across the cell membrane and act as a communication signal to mediate intercellular coupling. It binds to the regulator LuxR, and the LuxR–AHL complex undergoes a conformational change to form a transcriptional activator suitable for the *luxI* promoter binding to initiate gene expression. The ability to monitor these QS signal molecules would increase the understanding of microorganism communication. To date, quantification of bacterial AHLs has involved ultra-performance liquid chromatography, which is a complicated procedure [11]. Until recently, detecting QS-related signaling molecules from gram-negative bacteria has relied primarily on bacterial reporter systems [12]; ultrasensitive detection of QS molecules has been achieved in *Mesorhizobium huakuii* [13]. The most frequently used sensor bacterium, *CV026* [14], produces the characteristic purple pigment violacein in the presence of AHL. However, this process takes a relatively long period, and a rapid and convenient method for detecting signaling molecules would be more attractive.

There have been efforts to directly measure and visualize metabolites in cells by using fluorescent indicator proteins (FLIPs), which can be targeted to subcellular compartments to specifically analyze concentration changes within a compartment of an intact live cell [15]. FLIPs consist of a domain that specifically binds a ligand and is sandwiched between 2 variants of green fluorescent protein [typically cyan fluorescent protein (CFP) and yellow fluorescent protein (YFP)] [16]. The efficiency of fluorescence energy transfer between the two fluorophores is highly dependent on their distance from each other and orientation [17, 18]. A change in the FRET efficiency can be detected upon ligand binding, which induces a conformational change in the protein and alters the distance between the fluorophores. Recently, a number of bacterial periplasmic binding proteins, which undergo a conformational change upon ligand binding, have successfully been used to develop FRET nanosensors for glutamate, maltose, ribose, and glucose [19–22]. Besides periplasmic binding proteins, we developed recently a FRET-based biosensor using a regulatory domain GAF for tracking of 2-oxoglutarate in real-time [23], telling that a large range of proteins could be considered for sensor construction. An in vitro assay system has been described for the rapid detection and quantification of furanosyl borate diester (BAI-2) that belongs to the subclass autoinducer 2 (AI-2), a QS-related signaling molecule, based on the regulator protein LuxP [24]. In this study, we constructed a genetically encoded fluorescent biosensor of the QS signaling molecule 3OC6HSL that recruited the 3OC6HSL-binding regulator LuxR protein derived from the marine bacterium *V. fischeri*. We systematically engineered a linker moiety by inserting peptide connectors of different lengths. The resulting biosensor, QSflip, exhibited high selectivity to 3OC6HSL compared to related compounds. The sensor was also employed to determine 3OC6HSL concentrations both in vitro and in vivo.

Materials and Methods

Bacterial strains and reagents

Bacillus thuringiensis ATCC 10792 was cultured in Luria–Bertani (LB) medium at 30 °C. *E. coli* DH5α and BL21 (DE) cells were cultured in LB medium at 37 °C. For AiiA (GenBank Accession No.: ACI96342.1), AHL-lactonase expression in *E. coli* BL21 was induced by adding isopropyl β-D-1-thiogalactopyranoside (IPTG) and culturing at 30 °C. IPTG (1 mM) was used to induce AiiA gene expression. Antibiotics were used at the following concentrations: kanamycin at 50 μg/mL and chloramphenicol at 100 μg/mL. Autoinducer *N*-(3-oxo-hexanoyl)-L-homoserine lactone (3OC6HSL) was purchased from Sigma-Aldrich (St. Louis, MO, USA).

Construction of plasmids

We extracted the *B. thuringiensis* 4Q7 genome by using the BioDev genome extraction kit (Invitrogen^{TM}) with polymerase chain reaction analysis of the AHL-lactonase gene from the genome. The AiiA gene and a pET-28a plasmid were digested with *Eco*RI and *Xho*I for construction of the pET-28a/AiiA4Q7 plasmid. Four restriction sites *Bam*HI, *Eco*RI, *Sac*I, and *Sal*I in the pET-28a (+) vector were chosen for tandem fusion of YFP, LuxR (GenBank Accession No.: AAQ90231.1) and CFP to construct a FRET biosensor (Fig. S1 and Table S1). CFP and YFP (mutants of EGFP, GenBank Accession No.: U55762.1) were cloned from the commercially available plasmids pECFP-N1 (catalog #6900-1; Clontech, Mountain View, CA, USA) and pEYFP-N1 (catalog #6006-1; Clontech). *E. coli* DH5α was used as the cloning host, and *E. coli* BL21 (DE3) was used as the protein production host.

Protein expression, purification, and characterization

BL21(DE3) were grown at 30 °C in LB broth supplemented with 100 mg/L kanamycin. Protein expression was induced with 1 mM IPTG at an optical density (OD_{600}) of 0.6, and the

cells were grown for an additional 6 h. Bacterial cells were harvested by centrifugation, and the cell pellet was suspended in 50 mM phosphate-buffered saline (PBS; pH 8.0) before sonication. All analytes were dissolved in the same buffer and adjusted to a final pH 8.0. FLIPs were purified by His-binding affinity chromatography (Novagen, Madison, WI, USA). Binding to the resin was performed using the batch method at 4 °C for 4 h, washed in a column with 20 mM Tris–HCl and 20 mM Tris–HCl containing 20 mM imidazole at pH 8.0, and eluted with 250 mM imidazole in Tris–HCl (pH 8.0). Purified FLIP was dialyzed against 50 mM PBS (pH 8.0) before in vitro assays.

In vitro assays

Fluorescence was measured in a fluorescence microplate reader (Bio-Tek Instrument, Winooski, VT, USA) by using a black 96-well microplate (Fluotrac 200; Greiner Bio-One GmbH, Frickenhausen, Germany). Emission wavelengths of 478 and 528 nm or a continuous spectrum from 460 to 600 nm were monitored at an excitation wavelength of 440 nm. A blank measurement was obtained from a well containing only FLIP without the reaction chemical. Affinity constants (K_d) were determined by fitting the titration curves to a single-site-binding isotherm: $R = R_{apo} + (R_{sat-}R_{apo}) * X/(K_d + X)$ [16]. X, ligand concentration; R, ratio; R_{apo}, ratio in the absence of ligand; R_{sat}, ratio at saturation with ligand. All ratio values were derived from the averages of at least three titration experiments.

In vivo assays

Escherichia coli BL21 (DE3) were grown for 3 h in LB medium at 37 °C before induction by the addition of 0.5 mM IPTG overnight at 20 °C. Cultures were stored overnight at 4 °C and then suspended in carbon-free M9 medium (pH 8.0); 50 mg/L kanamycin sulfate was added to avoid outer interference [25]. Next, 100 μL of culture was transferred to 96-well plates. Fluorescence emission at 478 and 528 nm (excitation 440 nm, bandwidth 2 nm) were recorded in a in a fluorescence microplate reader (Bio-Tek Instrument) with shaking at 170 rpm between readings. 3OC6HSL and AiiA were manually added to the M9 media.

Results

Design and characterization of FRET-based sensor

Binding of a ligand to a promoter with varying levels of intensity causes intramolecular conformational changes, which is an important regulatory mechanism of gene expression [26, 27]. LuxR binds to AHL to form a LuxR–AHL complex, which is a transcriptional activator of the LuxI promoter [28]; this complex was used to construct a synchronized oscillator [29]. To monitor the binding of 3OC6HSL to LuxR, we fused a CFP and YFP to the LuxP protein to construct FRET-based biosensors.

To examine the usefulness of the FLIP3OC6HSL sensor, purified sensor protein was mixed with 3OC6HSL and excited at 440 nm. The emission spectra showed 2 peaks corresponding to CFP and YFP (Fig. 1a). Addition of 3OC6HSL resulted in an increase in CFP emission and a decrease in YFP emission, with a decreasing 528/478 nm ratio from 3.07 to 2.50. The ratio of YFP to CFP emission intensity changed upon addition of 3OC6HSL, demonstrating that the conformational change in the 3OC6HSL recognition domain LuxR resulted in a change in the FRET efficiency. Based on the decreased 528/478 nm ratio induced by 3OC6HSL binding, we hypothesized that 3OC6HSL caused a change in the LuxR domain to open the conformation from a relatively closed form and that the distance between the two fluorophores increased, resulting in a lower FRET efficiency (Fig. 1b). The sensor was mixed with 3OC6HSL at different concentrations and the data were fitted to a single site-binding curve as described in the "Methods" section. K_d was determined to be 1.9 mM (Fig. 1c); and the detection range was regarded to be 0.1–10 mM. To measure the specificity of FLIP3OC6HSL, we chose L-serine, L-homoserine, and L-homoserine lactone hydrochloride, which are analogs of 3OC6HSL, for analysis. Because the solubility of 3OC6HSL was 20 mM in PBS buffer, all ligands were determined at a final concentration of 10 mM, with FLIP3OC6HSL exhibiting high specificity (Fig. 1d).

Optimization for improved 3OC6HSL sensor

The C-terminal domain of the *V. fischeri* transcription activator LuxR, which represents the DNA-binding domain [30], was not thought to be involved in the conformational change. To construct a more effective nanosensor, we generated several sensors by using a truncated LuxR, N-terminal LuxR31–160 (autoinducer-binding domain), and LuxR1-221 (GenBank AAQ90231.1) by sequence alignment with the NCBI database. However, all nanosensors were inactive in inclusion bodies, indicating that LuxR has a rigid structure and changes in protein structure affect its folding. The distance and orientation between the two fluorophores determine the efficiency of energy transfer from CFP to YFP. To achieve a more effective nanosensor, a set of improved 3OC6HSL sensors was constructed by linker addition to the 3OC6HSL-binding domain LuxR with (Gly4Ser) as a linker

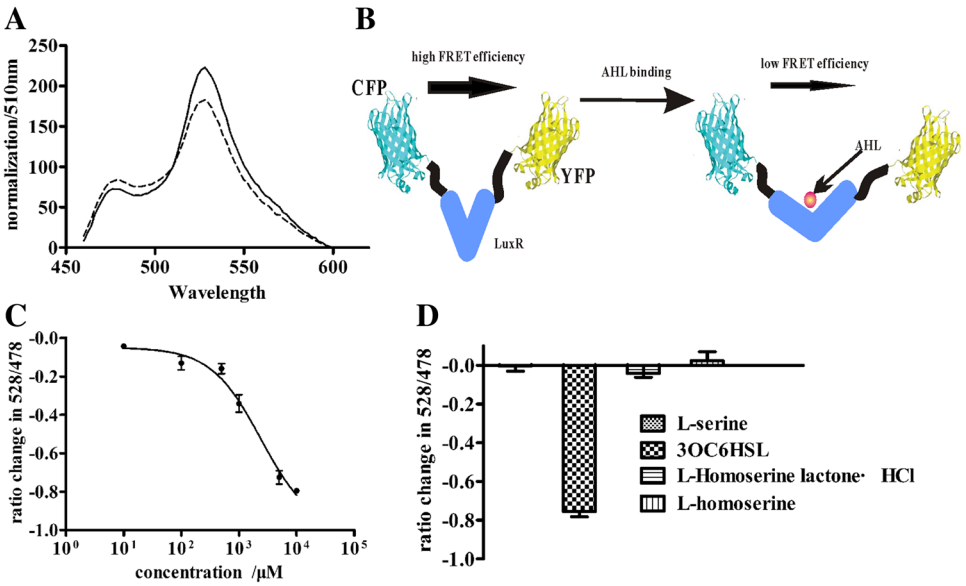

Fig. 1 Characterization of sensor in vitro. **a** Fluorescence emission spectrum of FLIP3OC6HSL with (*dotted line*) and without (*solid line*) 3OC6HSL. Purified FRET sensor FLIP3OC6HSL was analyzed, and the fluorescence emission was recorded at an excitation of 440 nm in a fluorescence plate reader. **b** Energy transfer illustration, 3OC6HSL binding caused a conformational change resulting in a decrease in energy transferred from CFP to YFP. **c** The emission ratio 528/478 nm was determined at different 3OC6HSL concentrations to monitor the binding curve. **d** The emission ratio of 528/478 nm was determined by using different ligands at concentrations of 10 mM. Changes in the FRET ratio are shown as absolute values. *Error bars* indicate standard deviations ($n = 3$)

Table 1 Primers used for constructing and engineering improved 3OC6HSL sensors

FLIP	Linker	Primer
FLIP3OC6HSL-1	LuxR-(Gly4Ser)2	TAAGAGCTCACTGCCACCTCCTCCGCTACCACCTCCTCCATTTTTAAAGTATGG
		TAAGAATTCAAAAACATAAATGCCGACGACA
FLIP3OC6HSL-2	LuxR-(Gly4Ser)3	TAAGAATTCAAAAACATAAATGCCGACGACA
		TAAGAGCTCACTACCACCTCCACCGCTTCCACCTCCTCCACTGCCGCCTCCCCCATTTTTAAAGTATGG
FLIP3OC6HSL-3	(Gly4Ser)2-LuxR-(Gly4Ser)3	TAAGAATTCGGCGGTGGCGGAAGTGGTGGTGGAGGAAGCAAAAACATAAATGCC
		TAAGAGCTCACTACCACCTCCACCGCTTCCACCTCCTCCACTGCCGCCTCCCCCCATTTTTAAAGTATGG
FLIP3OC6HSL-4	(Gly4Ser)3-LuxR-(Gly4Ser)3	TAAGAATTCGGTGGCGGTGGAAGCGGCGGTGGCGGAAGTGGCGGTGGCGGCAGCAAAAACATAAATGCC
		TAAGAGCTCACTACCACCTCCACCGCTTCCACCTCCTCCACTGCCGCCTCCCCCCATTTTTAAAGTATGG
FLIP3OC6HSL-5	(Gly4Ser)2-LuxR	TAAGAGCTCATTTTTAAAGTATGGGCAATCAATT
		TAAGAATTCGGCGGTGGCGGAAGTGGTGGTGGAGGAAGCAAAAACATAAATGCC
FLIP3OC6HSL-6	(Gly4Ser)3-LuxR	TAAGAATTCGGTGGCGGTGGAAGCGGCGGTGGCGGAAGTGGCGGTGGCGGCAGCAAAAACATAAATGCC
		TAAGAGCTCATTTTTAAAGTATGGGCAATCAATT

unit (Table 1). Of these nanosensors, FLIP3OC6HSL-4, FLIP3OC6HSL-5, and FLIP3OC6HSL-6 appeared to have a better ratio change, and FLIP3OC6HSL-6, referred to as QSflip, attained a 70 % Δratio increase in contrast with the original FLIP3OC6HSL (Fig. 2). All nanosensors exhibited similar K_d values. FLIP3OC6HSL-1, FLIP3OC6HSL-2, and FLIP3OC6HSL-3 showed a weaker response, indicating that distance and orientation between the 2 fluorophores was not consistent with the length of the linker.

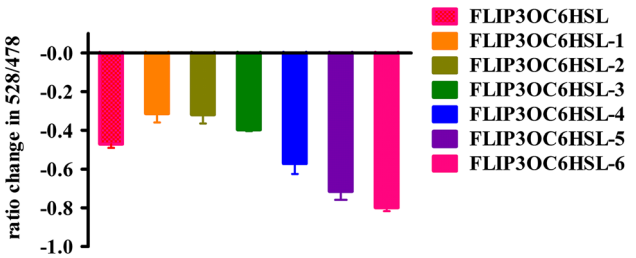

Fig. 2 Ratio change of 3OC6HSL sensors with 1 mM 3OC6HSL. All sensors were adjusted to protein concentrations of 9 μM before analysis

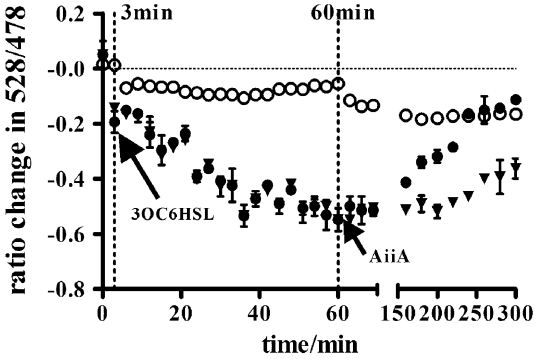

Fig. 3 Real-time monitoring of nanosensor responding to 3OC6HSL. 3OC6HSL dissolved in M9 was added at 3 min (*solid circle* and *closed triangle*), while AiiA (0.36 mg/mL) was added at 60 min (*solid circle*). *Error bars* indicate standard deviations ($n = 3$)

Monitoring of 3OC6HSL in *E. coli* cells

FRET sensors can be used to collect real-time data to study the kinetics of molecular accumulation. To test the in vitro ability of QSflip in *E. coli*, cells expressing QSflip in LB medium were transferred to M9 medium (pH 8.0) to prevent intrinsic fluorescence disturbance from LB medium. Fluorescence emission at 478 and 528 nm (excitation 440 nm, bandwidth 2 nm) were recorded using a fluorescence microplate reader (Fig. 3). When 3OC6HSL was added at 3 min, the 528/478 nm ration showed a slight decrease that was possibly due to the change in cell density. A time-dependent decrease in the ratio was detected in the experimental groups, whereas a decrease was observed in the control group. Addition of 3OC6HSL caused a sharp decrease in the ratio, indicating that 3OC6HSL can diffuse between *E. coli* cells very quickly and that sensor binding can be applied in vitro, with the FRET ratio reaching a steady state in approximately 60 min.

To monitor the dissociation of 3OC6HSL and the sensor, the AHL-hydrolyzing enzyme AiiA (Fig. S2) was added to experimental group (solid circles), while M9 buffer was added to the control group (hollow circles and closed triangles) at 60 min. Complete hydrolysis of 3OC6HSL occurred over approximately 4 h, as observed by a decrease in the FRET signal; this may be because the hydrolysis conditions were not ideal for the reaction to occur. As the hydrolysis reaction proceeded, the 3OC6HSL concentration declined, resulting in dissociation between the sensor and the molecule. Based on our data, binding between 3OC6HSL and QSflip is reversible. The ratio in the control group (closed triangles) showed mild recovery, in contrast with the experimental group (solid circles), indicating that 3OC6HSL is not stable in an aqueous solution or that the presence of *E. coli* accelerated 3OC6HSL degradation, but with a weaker capacity than that by AiiA.

Discussion

Visualizing and monitoring cellular activity in vivo with high spatial and temporal resolution is attractive because traditional analysis methods destroy living cells to extract metabolites of interest. Since the discovery of green fluorescent protein (GFP), scientists have used site-directed and random mutagenesis approaches to develop fluorescent protein mutants to create a family of proteins that nearly span the complete fluorescence spectrum. These fluorescent proteins have been used to construct genetically encoded fluorescent biosensors for optical imaging of biochemical and physiological functions in living cells [31], and these indicators allow noninvasive spatiotemporal tracing of intracellular metabolism.

In the present study, we developed a method for monitoring intracellular 3OC6HSL levels by using genetically encoded FRET-based biosensors based on the YFP to CFP

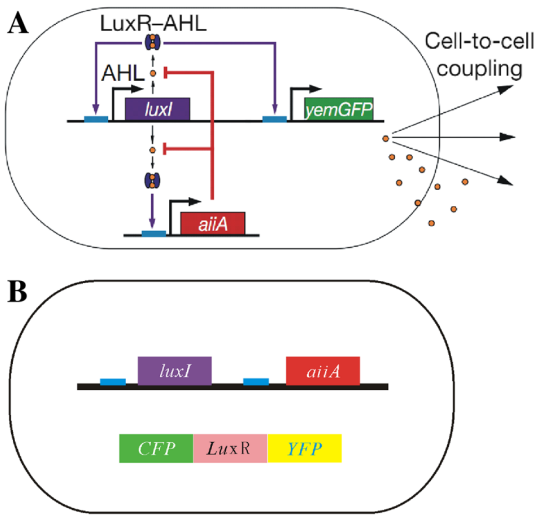

Fig. 4 Synchronized genetic network diagram. Intricate synchronized genetic clock design from Hasty (**a**), and potentially simplified design using the FLIP sensor (**b**)

ratio. The observed ligand-dependent decrease in the FRET ratio was associated with an intramolecular conformational change in the LuxR protein following ligand binding, possibly involving an increase in the distance between the N- and C-termini of LuxR or a rotation in LuxR to change the fluorophore dipole [32, 33]. With proper optimization, we developed a sensor suitable for visualizing 3OC6HSL both in vitro and in vivo.

QS systems are intensely examined in synthetic biology studies on various organisms [34, 35]. Recently, Hasty et al. [29] designed an intricate synchronized genetic clock employing AiiA and LuxR (Fig. 4a) and provided a specific model system for generating a mechanistic description of emergent coordinated behavior at the colony level. This system can be simplified using our genetic encoded sensor, QSflip, which was expressed in advance, and replaced the modular pluxI-yemGFP without the need for a degradation tag (Fig. 4b). This replaces the constitutively produced LuxR and serves as a constant in computational modeling.

Acknowledgments This study was supported by the China NSF (21276079), SRFDP (No. 20120074110009), the Key Grant Project (No. 313019) of the Chinese Ministry of Education, and the Fundamental Research Funds for the Central Universities.

References

1. Mattmann ME, Blackwell HE (2010) Small molecules that modulate quorum sensing and control virulence in *Pseudomonas aeruginosa*. J Org Chem 75:6737–6746
2. Yong YC, Zhong JJ (2013) Impacts of quorum sensing on microbial metabolism and human health. Adv Biochem Eng Biotechnol 131:25–61
3. Dos Reis Ponce A, Martins ML, de Araujo EF, Mantovani HC, Vanetti MC (2012) AiiA quorum-sensing quenching controls proteolytic activity and biofilm formation by *Enterobacter cloacae*. Curr Microbiol 65:758–763
4. Cech NB, Junio HA, Ackermann LW, Kavanaugh JS, Horswill AR (2012) Quorum quenching and antimicrobial activity of goldenseal (*Hydrastis canadensis*) against methicillin-resistant *Staphylococcus aureus* (MRSA). Planta Med 78:1556–1561
5. Mathesius U, Mulders S, Gao M, Teplitski M, Caetano-Anolles G, Rolfe BG, Bauer WD (2003) Extensive and specific responses of a eukaryote to bacterial quorum-sensing signals. Proc Natl Acad Sci U S A 100:1444–1449
6. Williams P (2002) Quorum sensing: an emerging target for antibacterial chemotherapy? Expert Opin Ther Targets 6:257–274
7. Kim JH, Lee SC, Kyeong HH, Kim HS (2010) A genetic circuit system based on quorum sensing signaling for directed evolution of quorum-quenching enzymes. ChemBioChem 11:1748–1753
8. Park SJ, Park SY, Ryu CM, Park SH, Lee JK (2008) The role of AiiA, a quorum-quenching enzyme from *Bacillus thuringiensis*, on the rhizosphere competence. J Microbiol Biotechnol 18: 1518–1521
9. Callahan SM, Dunlap PV (2000) LuxR- and acyl-homoserine-lactone-controlled non-lux genes define a quorum-sensing regulon in *Vibrio fischeri*. J Bacteriol 182:2811–2822
10. Lupp C, Urbanowski M, Greenberg EP, Ruby EG (2003) The *Vibrio fischeri* quorum-sensing systems ain and lux sequentially induce luminescence gene expression and are important for persistence in the squid host. Mol Microbiol 50:319–331
11. Thiel V, Vilchez R, Sztajer H, Wagner-Dobler I, Schulz S (2009) Identification, quantification, and determination of the absolute configuration of the bacterial quorum-sensing signal autoinducer-2 by gas chromatography–mass spectrometry. ChemBioChem 10:479–485
12. Yong YC, Zhong JJ (2009) A genetically engineered whole-cell pigment-based bacterial biosensing system for quantification of *N*-butyryl homoserine lactone quorum sensing signal. Biosens Bioelectron 25:41–47
13. Zhu J, Chai Y, Zhong Z, Li S, Winans SC (2003) *Agrobacterium* bioassay strain for ultrasensitive detection of *N*-acylhomoserine lactone-type quorum-sensing molecules: detection of autoinducers in *Mesorhizobium huakuii*. Appl Environ Microbiol 69:6949–6953
14. McClean KH, Winson MK, Fish L, Taylor A, Chhabra SR, Camara M, Daykin M, Lamb JH, Swift S, Bycroft BW, Stewart GS, Williams P (1997) Quorum sensing and *Chromobacterium violaceum*: exploitation of violacein production and inhibition for the detection of *N*-acylhomoserine lactones. Microbiology 143(Pt 12):3703–3711
15. Fehr M, Okumoto S, Deuschle K, Lager I, Looger LL, Persson J, Kozhukh L, Lalonde S, Frommer WB (2005) Development and use of fluorescent nanosensors for metabolite imaging in living cells. Biochem Soc Trans 33:287–290
16. Ewald JC, Reich S, Baumann S, Frommer WB, Zamboni N (2011) Engineering genetically encoded nanosensors for real-time in vivo measurements of citrate concentrations. PLoS ONE 6:e28245
17. Jares-Erijman EA, Jovin TM (2006) Imaging molecular interactions in living cells by FRET microscopy. Curr Opin Chem Biol 10:409–416
18. Piston DW, Kremers GJ (2007) Fluorescent protein FRET: the good, the bad and the ugly. Trends Biochem Sci 32:407–414
19. Fehr M, Frommer WB, Lalonde S (2002) Visualization of maltose uptake in living yeast cells by fluorescent nanosensors. Proc Natl Acad Sci U S A 99:9846–9851
20. Fehr M, Lalonde S, Lager I, Wolff MW, Frommer WB (2003) *In vivo* imaging of the dynamics of glucose uptake in the cytosol of COS-7 cells by fluorescent nanosensors. J Biol Chem 278: 19127–19133
21. Lager I, Fehr M, Frommer WB, Lalonde S (2003) Development of a fluorescent nanosensor for ribose. FEBS Lett 553:85–89
22. Okumoto S, Looger LL, Micheva KD, Reimer RJ, Smith SJ, Frommer WB (2005) Detection of glutamate release from neurons by genetically encoded surface-displayed FRET nanosensors. Proc Natl Acad Sci U S A 102:8740–8745
23. Zhang C, Wei ZH, Ye BC (2013) Quantitative monitoring of 2-oxoglutarate in *Escherichia coli* cells by a fluorescence resonance energy transfer-based biosensor. Appl Microbiol Biotechnol. doi:10.1007/s00253-013-5121-5
24. Rajamani S, Zhu J, Pei D, Sayre R (2007) A LuxP-FRET-based reporter for the detection and quantification of AI-2 bacterial quorum-sensing signal compounds. Biochemistry 46:3990–3997
25. Kaper T, Lager I, Looger LL, Chermak D, Frommer WB (2008) Fluorescence resonance energy transfer sensors for quantitative monitoring of pentose and disaccharide accumulation in bacteria. Biotechnol Biofuels 1:11
26. Sundaresan V, Yamaguchi M, Chartron J, Stout CD (2003) Conformational change in the NADP(H) binding domain of transhydrogenase defines four states. Biochemistry 42:12143–12153

27. Martinez SE, Heikaus CC, Klevit RE, Beavo JA (2008) The structure of the GAF A domain from phosphodiesterase 6C reveals determinants of cGMP binding, a conserved binding surface, and a large cGMP-dependent conformational change. J Biol Chem 283:25913–25919
28. Waters CM, Bassler BL (2005) Quorum sensing: cell-to-cell communication in bacteria. Annu Rev Cell Dev Biol 21:319–346
29. Danino T, Mondragon-Palomino O, Tsimring L, Hasty J (2010) A synchronized quorum of genetic clocks. Nature 463:326–330
30. Mel'kina OE, Manukhov IV, Zavil'gel'skii GB (2010) The C-terminal domain of the *Vibrio fischeri* transcription activator LuxR is not essential for degradation by Lon protease. Mol Biol (Mosk) 44:515–519
31. Miranda JG, Weaver AL, Qin Y, Park JG, Stoddard CI, Lin MZ, Palmer AE (2012) New alternately colored FRET sensors for simultaneous monitoring of Zn(2)(+) in multiple cellular locations. PLoS ONE 7:e49371
32. Ansbacher T, Srivastava HK, Stein T, Baer R, Merkx M, Shurki A (2012) Calculation of transition dipole moment in fluorescent proteins—towards efficient energy transfer. Phys Chem Chem Phys 14:4109–4117
33. Iqbal A, Arslan S, Okumus B, Wilson TJ, Giraud G, Norman DG, Ha T, Lilley DM (2008) Orientation dependence in fluorescent energy transfer between Cy3 and Cy5 terminally attached to double-stranded nucleic acids. Proc Natl Acad Sci U S A 105:11176–11181
34. Schmid N, Pessi G, Deng Y, Aguilar C, Carlier AL, Grunau A, Omasits U, Zhang LH, Ahrens CH, Eberl L (2012) The AHL- and BDSF-dependent quorum sensing systems control specific and overlapping sets of genes in *Burkholderia cenocepacia* H111. PLoS ONE 7:e49966
35. Perez-Montano F, Jimenez-Guerrero I, Contreras Sanchez-Matamoros R, Lopez-Baena FJ, Ollero FJ, Rodriguez-Carvajal MA, Bellogin RA, Espuny MR (2013) Rice and bean AHL-mimic quorum-sensing signals specifically interfere with the capacity to form biofilms by plant-associated bacteria. Res Microbiol 164:749–760